FEMS Microbes, 2, 2021, xtab004

doi: 10.1093/femsmc/xtab004
Advance Access Publication Date: 14 April 2021
Research Article

RESEARCH ARTICLE – Microbes & Metabolism

Twin-arginine translocation (Tat) mutants in *Salmonella enterica* serovar Typhimurium have increased susceptibility to cell wall targeting antibiotics

Adrienne M. Brauer[1,†], Alexandra R. Rogers[2] and Jeremy R. Ellermeier[2,*,‡]

[1]Department of Biology, Southeast Missouri State University, Cape Girardeau, MO 63701, USA and
[2]Department of Microbiology and Immunology, Midwestern University, 19555 N 59th Avenue, Glendale, AZ 85308, USA

*Corresponding author: 19555 N 59th Avenue, Glendale, AZ 85308, USA. E-mail: jeller@midwestern.edu

†Present address: Department of Biology, Washington University in St Louis, St Louis, MO 63130, USA.

One sentence summary: This work demonstrates the susceptibility of *tatABC* deletions to cell wall targeting antibiotics and determines which substrates are critical to this phenotype.

‡Jeremy R. Ellermeier, http://orcid.org/0000-0001-7704-7083

ABSTRACT

The twin-arginine translocation (Tat) system is a protein secretion system that is conserved in bacteria, archaea and plants. In Gram-negative bacteria, it is required for the export of folded proteins from the cytoplasm to the periplasm. There are 30 experimentally verified Tat substrates in *Salmonella*, including hydrogenase subunits, enzymes required for anaerobic respiration and enzymes involved in peptidoglycan remodeling during cell division. Multiple studies have demonstrated the susceptibility of *tat* mutants to antimicrobial compounds such as SDS and bile; however, in this work, we use growth curves and viable plate counts to demonstrate that cell wall targeting antibiotics (penicillins, carbapenems, cephalosporins and fosfomycin) have increased killing against a Δ*tat* strain. Further, we demonstrate that this increased killing is primarily due to defects in translocation of critical Tat substrates: MepK, AmiA, AmiC and SufI. Finally, we show that a Δ*hyaAB* Δ*hybABC* Δ*hydBC* strain has an altered Δ_ψ that impacts proper secretion of critical Tat substrates in aerobic growth conditions.

Keywords: stress response; tat; ampicillin

INTRODUCTION

Salmonella enterica serovar Typhimurium (S. Typhimurium) is a Gram-negative pathogen that causes an array of diseases in a variety of hosts. In humans, S. Typhimurium causes self-limiting gastroenteritis in otherwise healthy individuals; however, in immunocompromised or otherwise susceptible hosts, S. Typhimurium can cause life-threatening system infection (Mastroeni and Grant 2011). Systemic salmonellosis has historically been treated with ampicillin and ciprofloxacin; however, the emergence of resistant strains has led to the use of cephalosporins in recent years (Gal-Mor, Boyle and Grassl 2014). Penicillins and cephalosporins work by irreversibly binding the enzyme transpeptidase, preventing the synthesis of peptidoglycan during cell division. Use and overuse of these

Received: 14 January 2021; **Accepted:** 1 April 2021

Table 1. *Salmonella enterica* serovar Typhimurium Tat substrates. Adapted from Craig *et al.* (2013) and Sargent, Berks and Palmer (2010).

Molybdopterin-independent Tat substrates		
Protein	*Functional knockout*	*Substrate function*
AslA (STM0084)	Δ*aslA*	*Acid-inducible sulfatase*
Mig5 (PSLT046)	Δ*mig5*	*Carbonic anhydrase*
CueO	Δ*cueO*	*Multicopper oxidase*
FhuD	Δ*fhuD*	*Fe^{3+} hydroxamate siderophore transport component*
HyaA	Δ*hyaAB*	*Hydrogenase 1 small subunit*
HybA	Δ*hybABC*	*Hydrogenase 2 subunit*
HypO	Δ*hybABC*	*Hydrogenase 2 small subunit*
HydA	Δ*hydBC*	*Hydrogenase 5 small subunit*
MdoG	Δ*mdoG*	*Glucan biosynthesis*
WcaM	Δ*wcaM*	*Colanic acid biosynthesis*
NrfC	Δ*nrfA*	*Nitrite reductase*
MepK (YcbK)	Δ*mepK*	*3–3 DAP murein endopeptidase*
AmiA	Δ*amiA*	*N-Acetylmuramoyl-L-alanine amidase*
AmiC	Δ*amiC*	*N-Acetylmuramoyl-L-alanine amidase*
SufI (FtsP)	Δ*sufI*	*Cell division protein*
Molybdopterin-dependent Tat substrates		
Protein	*Functional knockout*	*Substrate function*
STM0611	Δ*moaDE*	*Putative oxidoreductase*
DmsA	Δ*moaDE*	*Dimethyl sulfoxide reductase, subunit A*
DmsA1	Δ*moaDE*	*Dimethyl sulfoxide reductase, subunit A*
DmsA2	Δ*moaDE*	*Dimethyl sulfoxide reductase, subunit A*
TtrA	Δ*moaDE*	*Tetrathionate reductase, subunit A*
TtrB	Δ*moaDE*	*Tetrathionate reductase, subunit B*
YnfF	Δ*moaDE*	*Putative anaerobic reductase*
YnfE	Δ*moaDE*	*Putative anaerobic reductase*
FdnG	Δ*moaDE*	*Formate dehydrogenase N, alpha subunit*
PhsA	Δ*moaDE*	*Thiosulfate reductase*
NapG	Δ*moaDE*	*Quinol dehydrogenase*
NapA	Δ*moaDE*	*Nitrate reductase, large subunit*
YedY	Δ*moaDE*	*Sulfoxide reductase*
TorA	Δ*moaDE*	*TMAO reductase*
FdoG	Δ*moaDE*	*Formate dehydrogenase O, alpha subunit*

antibiotics have led to an increase of multidrug-resistant isolates of *Salmonella* species (Mather *et al.* 2013; Krueger *et al.* 2014; Nair, Venkitanarayanan and Kollanoor Johny 2018), hastening the need to develop new and alternative treatment methods.

The twin-arginine translocation (Tat) system is a protein secretion system present in the cytoplasmic membrane of many bacteria and archaea. In Gram-negative organisms, the Tat translocon transports substrate proteins from the cytoplasm to the periplasmic space where the protein can undergo further export out of the cell or remain in the periplasm. Substrates of Tat are typically proteins that must be folded in the cytoplasm, often because they contain essential cofactors that are limiting in the periplasmic space (Palmer, Sargent and Berks 2005; Palmer and Berks 2012). About half of the known Tat substrates in *S.* Typhimurium are dependent on molybdopterin as a cofactor (Sargent, Berks and Palmer 2010). The Tat export process is independent of ATP, using proton motive force (PMF) to drive translocation (Yahr and Wickner 2001; Alami *et al.* 2002). The secretion complex is made of three proteins: TatA or TatE, TatB and TatC (Berks, Palmer and Sargent 2003; Orriss *et al.* 2007; Palmer and Berks 2012). The Tat export complex components assemble at the cytoplasmic membrane. Data suggest that either TatA or TatE is recruited to a TatB/TatC complex bound to a Tat substrate. TatA and TatE seem to form translocation channels for the substrate (Gohlke *et al.* 2005; Leake *et al.* 2008). Tat is named after the N-terminal twin-arginine signal sequence commonly associated with secretion targets. The main structural components of the Tat system are encoded in the three-gene *tatABC* operon (Jack *et al.* 2001). TatD, transcribed independently, seems to play a role in repairing hydrogen peroxide-mediated DNA damage (Chen *et al.* 2014). TatE, also encoded separately from other Tat complex proteins, is functionally equivalent to TatA (Jack *et al.* 2001).

Secreted proteins carry the twin-arginine signal sequence that binds to the translocon and initiates movement to the periplasm (Berks 1996; Berks, Sargent and Palmer 2000; Palmer, Sargent and Berks 2005). Loss of the Tat system is not lethal to *S.* Typhimurium; however, there are pleiotropic effects on metabolism, virulence and proper cell envelope development (Berks, Palmer and Sargent 2003; Rollauer *et al.* 2012; Craig *et al.* 2013). Tat mutants are also more susceptible than wild-type *S.* Typhimurium to antimicrobial agents, such as SDS and bile (Ize *et al.* 2003; Pradel *et al.* 2009; Reynolds *et al.* 2011).

The total number of Tat substrates varies by species. *Salmonella* Typhimurium has 30 proteins that are substrates of Tat, either predicted with bioinformatics or experimentally confirmed (Craig *et al.* 2013). These Tat substrates include enzymes necessary for anaerobic respiration, hydrogenases and cell wall amidases, among others (Table 1). Indeed, the Tat system has been shown to be critical for the virulence of *S.* Typhimurium and other pathogenic species (Caldelari *et al.* 2006; Lavander *et al.* 2006; Reynolds *et al.* 2011; Craig *et al.* 2013; Fujimoto *et al.* 2018)

while not being essential for *in vitro* growth. In S. Typhimurium, this virulence defect is due to the combined loss of three genes: *amiA*, *amiC* and *sufI* (Craig *et al.* 2013; Fujimoto *et al.* 2018). AmiA and AmiC are *N*-acetylmuramyl-L-alanine amidases that remove cross-links in peptidoglycan during cell division (Heidrich *et al.* 2001; Bernhardt and De Boer 2003), while SufI (FtsP) is important for stabilization of the divisome during stress conditions (Heidrich *et al.* 2001; Samaluru, Saisree and Reddy 2007; Tarry *et al.* 2009). Interestingly, in *Escherichia coli*, overproduction of a third amidase not secreted via Tat, AmiB, is able to compensate for the deletion of *tatC* (Ize *et al.* 2003). Overproduction of AmiA or AmiC does not provide the same benefit for *E. coli* (Ize *et al.* 2003). Indeed, overproduction of Tat substrates in a Tat^+ background is actually detrimental to the cell as it prevents efficient translocation of Tat substrates (DeLisa *et al.* 2004). MepK (formerly YcbK) is an endopeptidase that cleaves mDAP–mDAP cross-links (Chodisetti and Reddy 2019) and deletion of *mepK* also causes a virulence defect in mice (Craig *et al.* 2013). The combined data from *E. coli* and S. Typhimurium demonstrate a critical role of the Tat system in maintenance of the Gram-negative cell envelope. Strains deleted for genes encoding the Tat apparatus experience several growth phenotypes, including elongated cells and septal defects during division (Heidrich *et al.* 2001; Samaluru, Saisree and Reddy 2007).

In this study, we demonstrate that the deletion of *tatABC* is significantly more susceptible to low levels of cell wall targeting antibiotics as compared with wild type. Further, we show that susceptibility is primarily due to loss of specific substrates MepK, AmiA, AmiC and SufI, which all play critical roles in maintenance of peptidoglycan. Our data also suggest an important role for hydrogenases in aerobic growth, as a Δ*hyaAB* Δ*hybABC* Δ*hydBC* strain has an altered Δ_Ψ that likely leads to inefficient translocation of critical Tat substrates.

MATERIALS AND METHODS

Media, reagents and enzymatic assays

Luria–Bertani (LB) medium was used in all experiments for growth of bacteria and SOC was used for the recovery of transformants (Maloy *et al.* 1996). Bacterial strains were routinely grown at 37°C except for strains containing the temperature-sensitive plasmids, pCP20 or pKD46, which were grown at 30°C. Antibiotics were used at the following concentrations for selection purposes: 50 μg/mL ampicillin (Amp); 20 μg/mL chloramphenicol (Cm); and 50 μg/mL kanamycin (Km). Enzymes were purchased from New England BioLabs and were used according to the manufacturer's recommendations. Primers and gBlocks gene fragments were purchased from Integrated DNA Technologies (San Diego, CA, USA). Antibiotics were purchased from MilliporeSigma (St. Louis, MO, USA).

Growth curves and viable plate counts

Growth curves were performed in 96-well plates. Briefly, overnight cultures were subcultured 1:100, grown for 6 h and then subcultured 1:100 again into medium for the growth curve. Four independent replicates were grown in LB with appropriate antibiotics and concentrations. Growth curves were performed in a temperature-controlled BioTek Cytation 3 plate reader at 37°C with 200 r.p.m. of agitation. OD_{600} readings were taken every 15 min. The median for each time point was plotted with standard deviation. Column 1 is always the uninoculated, LB only negative control. After 14 h, serial dilutions were performed in LB and 10 μL spot plated on non-selective LB agar to determine viable cells/mL.

Measurement of Δ_Ψ with flow cytometry

BacLight Bacterial Membrane Potential Kit purchased from ThermoFisher Scientific (Waltham, MA, USA) was used for solutions of $DiOC_2(3)$ carbocyanine dye (3,3′-diethyloxacabocyanine iodide) and CCCP (carbonyl cyanide 3-chlorophenylhydrazone). Stationary cultures were diluted 1:100 in 1× PBS. $DiOC_2(3)$ was added to final concentration of 30 μM. A depolarized control was running with the addition of CCCP with the final concentration of 5 μM. Samples were incubated for 30 min at 37°C, then data were collected on a BioRad S3e cell sorter. Mean fluorescence intensity (MFI) was calculated with a derived parameter utilizing the following formula for each event: red fluorescence − green fluorescence + 500, where 500 is a constant used to ensure that all ratiometric values are positive. Then, the geometric mean is generated for each independent run based on 10 000 events.

Fluorescent microscopy

pAT5 (pBR322::TorA–GFP) was transformed into strains via electroporation. A single colony from an LB with ampicillin plate was suspended in water to create a bacterial smear on a glass slide; coverslip was mounted with 2% agarose. Slide was then visualized on Nikon Eclipse Ci-L microscope with Nikon DS-Fi3 color camera and NIS-Elements software using 100× objective and an EGFP filter.

Strain and plasmid construction

Bacterial strains and plasmids are described in Table 1. All *S. enterica* serovar Typhimurium strains used in this study are isogenic derivatives of the strain ATCC 14028 (American Type Culture Collection) and were constructed using P22 HT105/1 *int*-201 (P22)-mediated transduction (Maloy *et al.* 1996). Deletion of various genes and concomitant insertion of an antibiotic resistance cassette was carried out using Lambda Red-mediated recombination as described (Datsenko and Wanner 2000). In all cases, the appropriate insertion of the antibiotic resistance marker was checked by P22 linkage to known markers and/or polymerase chain reaction (PCR) analysis. The constructs resulting from this procedure were moved into a clean wild-type background (14028) by P22 transduction. In some strains, the antibiotic resistance cassettes were removed using the temperature-sensitive plasmid pCP20 carrying the FLP recombinase (Cherepanov and Wackernagel 1995). *Salmonella enterica* serovar Enteritidis (S. Enteritidis; ATCC 13076) and *Salmonella enterica* serovar Heidelberg (S. Heidelberg; ATCC 8326) were purchased from the American Type Culture Collection (Manassas, VA, USA). The Δ*tatABC11*::Kn allele initially generated in ATCC 14028 was moved into ATCC 8326 and ATCC 13076 via modified P22 transduction as previously reported (Edwards, Helm and Maloy 1999) with the modification of pretreatment of recipient cells at 45°C for 25 min. Constructs containing the OmpA signal sequence were designed and ordered as gBlocks fragments from Integrated DNA Technologies. Sequences are included in the Supporting Information. Oligos were used to amplify the fragments and clone into pBAD33 with appropriate restriction enzymes. Plasmids constructed in this work were verified by sequencing analysis at the Arizona State University Genomics Facility (Tempe, AZ, USA). Primers used for cloning and deletions are described in Table S2 (Supporting Information).

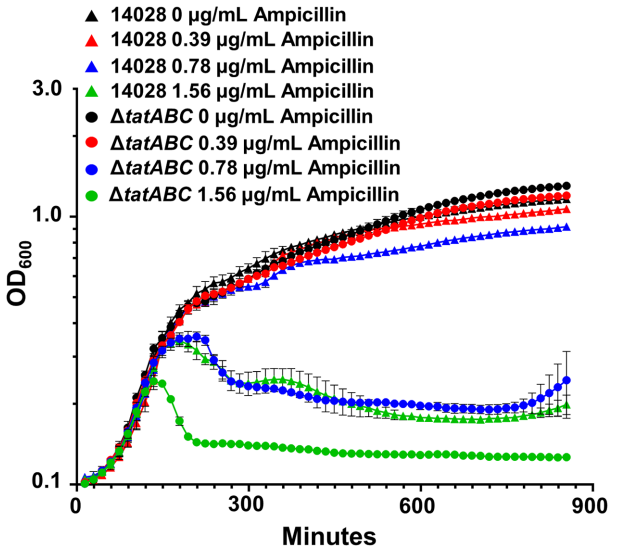

Figure 1. Δ*tatABC* is more susceptible to ampicillin than wild-type *S.* Typhimurium 14028. Strains were grown in LB with indicated concentrations of ampicillin and OD_{600} monitored over 14 h. Strains used were ATCC 14028 and JRE 140.

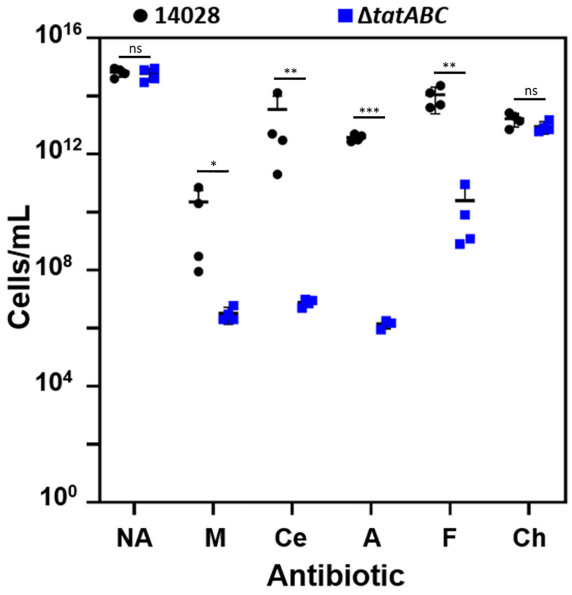

Figure 2. Δ*tatABC* is more susceptible than wild-type *S.* Typhimurium 14028 to peptidoglycan targeting antibiotics. Strains were grown in LB with indicated concentrations of ampicillin and OD_{600} monitored over 14 h. After 14-h growth curves in indicated antibiotics, strains were diluted and plated on non-selective LB to determine viable plate counts. NA: no antibiotic; M: 0.0313 μg/mL meropenem; Ce: 0.0625 μg/mL ceftriaxone; A: 0.78 μg/mL ampicillin; F: 1.0 μg/mL fosfomycin; Ch: 0.313 μg/mL chloramphenicol. Strains used were ATCC 14028 and JRE 140. Significance was determined using unpaired *t*-tests: $^{*}P < 0.05$; $^{**}P < 0.01$; $^{***}P < 0.001$.

RESULTS AND DISCUSSION

Low concentrations of ampicillin readily kill a Δ*tatABC* strain

With the effects of bile, SDS and other compounds that disrupt the cell envelope on *tat* mutants (Ize *et al.* 2003; Pradel *et al.* 2009; Reynolds *et al.* 2011), we predicted that peptidoglycan targeting antibiotics would also have a stronger effect on a Δ*tat* strain as compared with wild-type *S.* Typhimurium. We determined the effects of ampicillin and other cell wall targeting antibiotics using growth curves. The data (Fig. 1) show that deletion of *tatABC* causes *S.* Typhimurium to be more susceptible to low concentrations of ampicillin. Even 0.78 μg/mL of ampicillin, which has no impact on the final OD_{600} of wild-type *S.* Typhimurium, caused a 5-fold decrease in final OD_{600} of the Δ*tatABC* strain. Several previous studies have noted the elongated cell phenotype associated with deletion of *tat* genes and some Tat substrates (Heidrich *et al.* 2001; Stanley *et al.* 2001; Craig *et al.* 2013). We predicted the elongated cells and chains formed by cell division defects associated with Δ*tatABC* could be artificially elevating the OD_{600} of our cultures; thus, we did serial dilutions and spot plating to determine the viable cells/mL after the 14-h growth curve. The major benefit of this dual approach is that low concentrations of ampicillin do indeed kill the Δ*tatABC* strain readily; however, we saw spontaneous resistant mutants develop at low ampicillin concentrations. These manifest as a recovery in growth late in the curve with large error bars. The raw data show that in these cases, one of the four replicates grew to an optical density far higher the rest. Thus, using growth curves allows us to verify that strains have remained ampicillin sensitive and using viable plate counts gives an accurate read of cell viability, unaltered by the elongated cell phenotype associated with Δ*tatABC*. While we are reporting only viable plate counts in most cases, these were indeed taken from the end of 14-h growth curves.

Viable plate counts show that ampicillin causes a 1 000 000-fold decrease in viability of Δ*tatABC* as compared with wild type (Fig. 2B). Other peptidoglycan targeting antibiotics have similar effects. Ceftriaxone (1 000 000-fold), meropenem (10 000-fold) and fosfomycin (10 000-fold) all have a much more dramatic effect on the viability of the Δ*tatABC* strain as compared with wild type. To demonstrate that this phenotype is specific to antibiotics targeting the production of peptidoglycan, we included chloramphenicol as a control. The data show that there is no significant difference between Δ*tatABC* and wild-type 14028 in chloramphenicol sensitivity. Since these antibiotics all work by preventing peptidoglycan synthesis, we used ampicillin as a proxy to study the effect of cell wall targeting antibiotics on the Tat system.

The ampicillin effect on *tatABC* deletions is not serovar specific

To determine whether the effect of ampicillin on Δ*tatABC* is specific to *S.* Typhimurium, we purchased *S.* Enteritidis and *S.* Heidelberg from the ATCC. The Δ*tatABC* allele was moved from *S.* Typhimurium into *S.* Enteritidis and *S.* Heidelberg via modified P22 transduction and growth curves were performed to determine the effects of ampicillin. The data (Fig. 3) show that deletion of *tatABC* has a similar phenotype in *S.* Enteritidis and *S.* Heidelberg. While the concentrations of ampicillin that give a Δ*tatABC* phenotype in *S.* Enteritidis (1.56 ug/mL) and *S.* Heidelberg (3.125 ug/mL) are higher than *S.* Typhimurium (0.78 ug/mL), the general effect of ampicillin on the Δ*tatABC* strains is otherwise similar. Both serovars demonstrate ~1000-fold increased susceptibility of the Δ*tatABC* strains as compared with their wild-type counterparts. While the 1000-fold effect on serovars Heidelberg and Enteritidis is less dramatic than the 1 000 000-fold impact on Typhimurium, the general trend holds. It is difficult to speculate as to why the phenotype is less severe in these

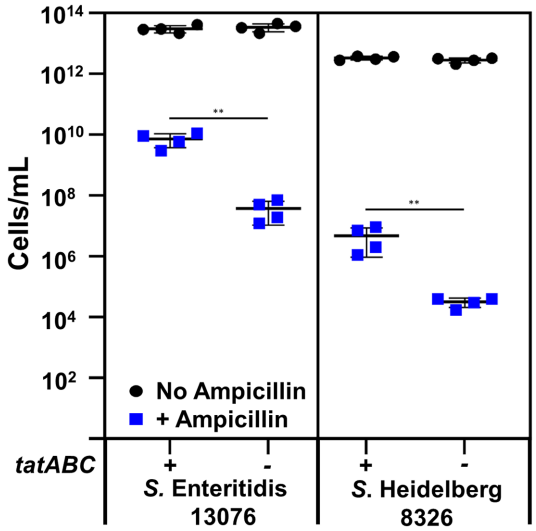

Figure 3. Δ*tatABC* is more readily killed by ampicillin than wild-type *S.* Enteritidis and *S.* Heidelberg. Strains were grown in LB with indicated concentrations of ampicillin and OD_{600} monitored over 14 h. After 14-h growth curves in indicated concentration of ampicillin, strains were diluted and plated on non-selective LB to determine viable plate counts. Strains used were ATCC 13076, ATCC 8326, JRE 423 and JRE 431. Significance was determined using unpaired *t*-tests: $^{*}P < 0.05$; $^{**}P < 0.01$; $^{***}P < 0.001$.

serovars; nonetheless, these data suggest that the phenotype would be applicable to other *S. enterica* serovars not tested.

The ampicillin effect on Δ*tatABC* is primarily due to loss of MepK, AmiA, AmiC and SufI

The Tat system has 30 substrates in *Salmonella* that have been identified via bioinformatics or experimentally (Craig *et al.* 2013); for the full list of Tat substrates, see Table 1. We predicted that growth defect of the Δ*tatABC* mutant in ampicillin was due to loss of specific substrates important in biogenesis and maintenance of the cell wall: AmiA, AmiC, MepK and SufI. AmiA and AmiC are amidases that remove cross-links in peptidoglycan during cell division (Heidrich *et al.* 2001; Bernhardt and De Boer 2003), while SufI is involved in stabilizing divisome (Heidrich *et al.* 2001; Tarry *et al.* 2009) during replication. MepK is a murein endopeptidase that cleaves 3–3 DAP cross-links in *E. coli* (Chodisetti and Reddy 2019).

We tested functional deletions of all known Tat substrates using growth curves and viable plate counts in LB alone and LB with 0.78 μg/mL of ampicillin. We individually deleted genes encoding each of the molybdopterin-independent Tat substrates, while a deletion of *moaDE* knocks out biosynthesis of the molybdopterin cofactor required by half of the Tat substrates that are involved in anaerobic respiratory pathways (Table 1). Thus, Δ*moaDE* is used as a single test to determine whether molybdopterin-requiring Tat substrates have an ampicillin phenotype. The data (Fig. 4) demonstrate that several Tat substrates have modest viability phenotypes in ampicillin as compared with wild-type 14028. A deletion of *cueO* shows a slight decrease in overall growth in 0.78 μg/mL of ampicillin, though the difference compared with 14028 wild type is not statistically significant. Figure 4 shows that any difference in growth and viability in Δ*moaDE* as compared with wild-type 14028 is statistically insignificant; therefore, none of the molybdopterin-requiring Tat substrates are impacted by the presence of ampicillin. A deletion of *frdA* had a notable growth defect in plain LB and a very modest difference compared with wild-type 14028 when treated with ampicillin; however, given the lack of difference between the LB control and the LB with ampicillin treatment, we did not follow up further. A single deletion of *mig5* and a triple deletion of hydrogenase subunits (Δ*hyaAB* Δ*hybABC* Δ*hydBC*) had significant phenotypes in ampicillin. These will be discussed further in another section.

Deletions of *amiA*, *amiC*, *sufI* and *mepK* cause more dramatic, significant phenotypes (Fig. 4). Given the apparent redundancy of AmiA and AmiC functions, we made an *amiA amiC* double-deletion strain and predicted that this double deletion would have a more substantial ampicillin phenotype. The data demonstrate that the Δ*amiA* Δ*amiC* strain is ~10-fold more attenuated than the single-deletion constructs and the difference between the single *amiA* and *amiC* deletions and the *amiA amiC* double deletion is significant (Fig. 4). Data from Craig *et al.* (2013) demonstrate the importance of AmiA, AmiC and SufI, but the authors only briefly note the significant 3-fold effect of the *ycbK* (*mepK*) deletion. Given the apparent importance of AmiA, AmiC, SufI and MepK, we constructed an Δ*amiA* Δ*amiC* Δ*sufI* Δ*mepK* quadruple deletion strain. Indeed, the viable plate counts show that the quadruple deletion is statistically equivalent to the Δ*tatABC* strain (Fig. 4).

There seems to be no reason for AmiA, AmiC and SufI to be exported specifically via Tat, as they are not predicted to have a required cofactor that is absent in the periplasm like other Tat substrates. Other work has demonstrated some flexibility in translocation of AmiA, AmiC and SufI using the Sec pathway even with their native Tat signal sequences (Tullman-Ercek *et al.* 2007). Additionally, *E. coli* AmiB is secreted via the Sec pathway rather than Tat and overproduction of AmiB compensates for a *tat* deletion (Heidrich *et al.* 2001). We overexpressed native AmiA, AmiC and SufI via pBAD33 and none of the substrates complemented the *tatABC* deletion (Fig. S1, Supporting Information). This result was expected given that with no functioning Tat system AmiA, AmiC and SufI would have to be exported via Sec. While there may be some flexibility in the pathway used for localization of these three substrates (Tullman-Ercek *et al.* 2007), any export of Tat substrates via Sec is clearly not efficient. Further, the data show that overproduction of AmiC and AmiA cause 10-fold and 100-fold decreases in viability of 14028, respectively, as compared with the pBAD33 empty vector control (Fig. S1, Supporting Information). Overproduction of SufI in the 14028 background has no impact on viability. This fits with previous work demonstrating that overproduction of Tat substrates can block efficient translocation via the Tat system (DeLisa *et al.* 2004) and we likely see that reflected in stunted growth in ampicillin when AmiA and AmiC are overproduced.

AmiA, AmiC and SufI exported via Sec complement Δ*tatABC*

Critical Tat substrates MepK, AmiA, AmiC and SufI were engineered to have the OmpA signal sequence for the Sec pathway ($OmpA_{1-21}$) replacing the native Tat signal sequence. The resulting constructs ($OmpA_{1-21}$-$AmiC_{32-418}$; $OmpA_{1-21}$-$AmiA_{35-290}$; $OmpA_{1-21}$-$SufI_{28-471}$; $OmpA_{1-21}$-$MepK_{31-183}$) were cloned into pBAD33 for expression in the Δ*tatABC* background. For shorthand purposes, we have named these constructs SecSP (Sec Signal Peptide)-substrate. The data show that overproduction of SecSP-AmiA, SecSP-AmiC and SecSP-SufI each compensate for the *tatABC* deletion (Fig. 5). Each construct increased growth of the Δ*tatABC* strain in the presence of ampicillin by ~1000-fold,

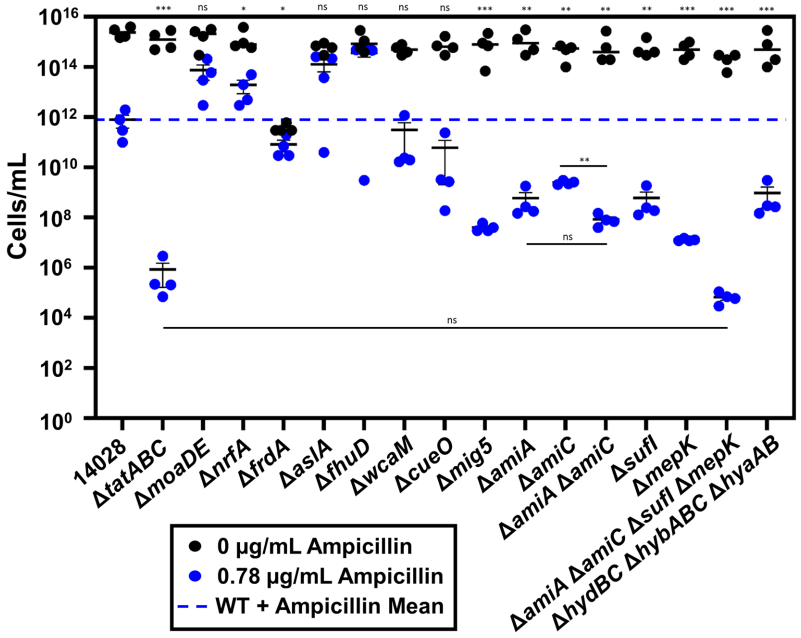

Figure 4. MepK, AmiA, AmiC and SufI account for most of the Δ*tatABC* phenotype in ampicillin. Mig5 also plays a significant role. Strains were grown in LB with indicated concentrations of ampicillin and OD_{600} monitored over 14 h. After 14-h growth curves in indicated concentration of ampicillin, strains were diluted and plated on non-selective LB to determine viable plate counts. Strains used were ATCC 14028, JRE 140, JS 1189 through JS 2004, JRE 507 and JRE 509. Significance was determined using unpaired *t*-tests: $^{*}P < 0.05$; $^{**}P < 0.01$; $^{***}P < 0.001$.

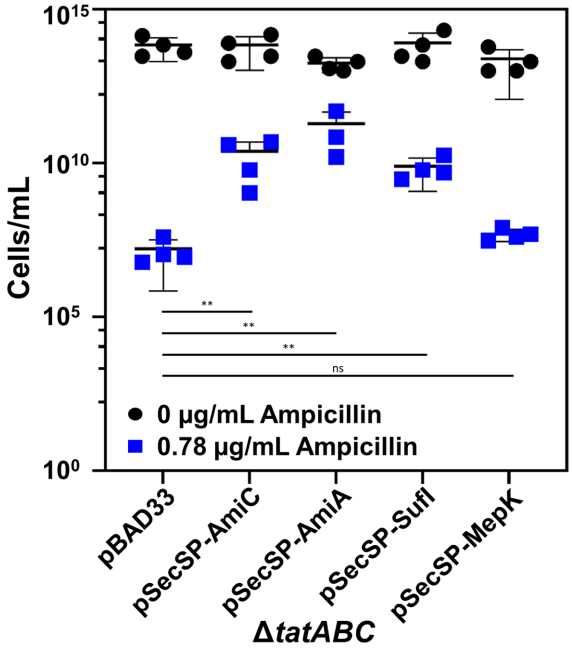

Figure 5. AmiA, AmiC and SufI exported via Sec complement the Δ*tatABC* phenotype in ampicillin. Strains were grown in LB with 0.2% arabinose and indicated concentrations of ampicillin and OD_{600} monitored over 14 h. After 14-h growth curves in indicated concentration of ampicillin, strains were diluted and plated on non-selective LB to determine viable plate counts. Strains used were JRE 458, JRE 460 JRE 462, JRE 464 and JRE 530. Significance was determined using unpaired *t*-tests: $^{*}P < 0.05$; $^{**}P < 0.01$; $^{***}P < 0.001$.

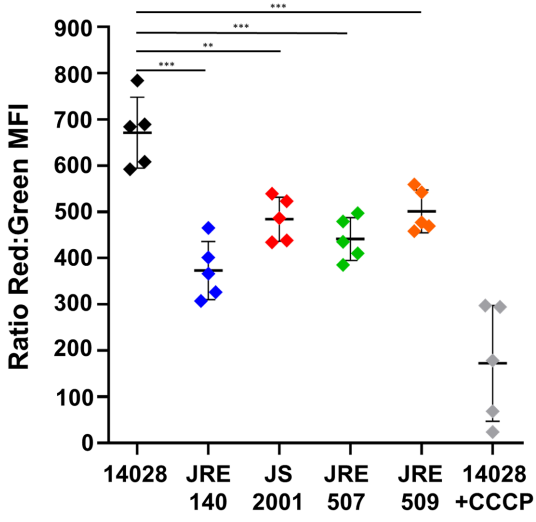

Figure 6. Hydrogenase deletion strain has altered Δ_ψ. Each diamond represents the MFI of 10 000 events from a single biological replicate. Strains used were JRE 104 (ATCC 14028), JRE 140 (Δ*tatABC*), JS 2001 (Δ*mig5*), JRE 507 (Δ*amiA* Δ*amiC* Δ*sufI* Δ*mepK*) and JRE 509 (Δ*hydBC* Δ*hybABC* Δ*hyaAB*). Significance was determined using unpaired t-tests: $^{*}P < 0.05$; $^{**}P < 0.01$; $^{***}P < 0.001$.

demonstrating the importance of these enzymes involved in peptidoglycan remodeling. In contrast, SecSP-MepK did not complement Δ*tatABC*; however, this is not surprising since MepK contains Zn^{2+} as a critical cofactor and likely must be exported via Tat after folding. Indeed, previous work has demonstrated that CueO with a Sec signal sequence is non-functional and it must be translocated from the cytoplasm via Tat in a partially folded state (Stolle, Hou and Brüser 2016).

It is interesting that overproduction and export via Sec of SecSP–AmiA, SecSP–AmiC or SecSP–SufI all compensate for the deletion of *tatABC* given the very different roles of AmiA/AmiC and SufI in the cell. Previous studies have shown that β-lactam antibiotics not only irreversibly bind PBPs but also induce a futile cycle that leads to disruption of cell wall synthesis machinery (Cho, Uehara and Bernhardt 2014). Given these data, it is

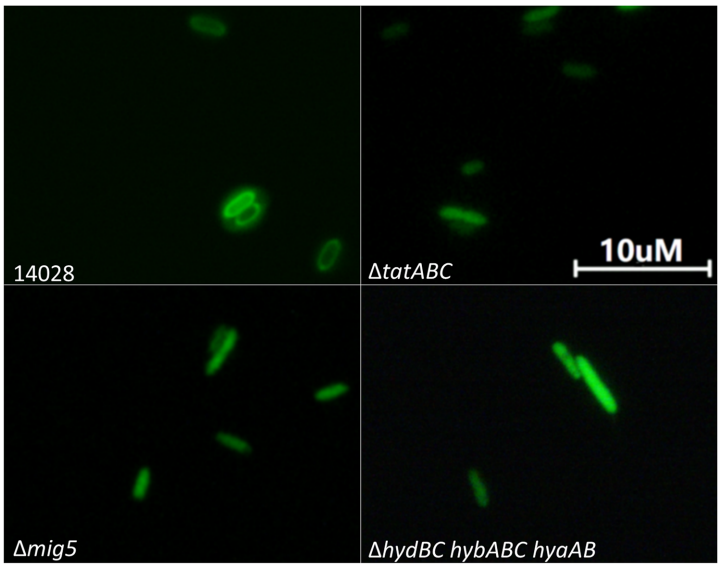

Figure 7. The Δ*hydBC* Δ*hybABC* Δ*hyaAB* strain does not efficiently export Tat substrates. Fluorescent microscopy shows that wild-type 14028 localizes TorA–GFPuv to the periplasmic space, while deletions of *tatABC*, *mig5* and *hydBC hybABC hyaAB* all localize TorA–GFPuv to the cytoplasm. Strains used were JRE 611 through JRE 614.

likely that deletion of Tat exacerbates the futile cycle induced by β-lactams and overproduction of even one key peptidoglycan-modifying enzyme relieves it. It is worth noting that fosfomycin disrupts formation of peptidoglycan by acting on MurA, a UDP-*N*-acetylglucosamine enolpyruvyl transferase that is essential in *E. coli* (Brown *et al.* 1995). Though fosfomycin and β-lactams target peptidoglycan via different mechanisms, they have a similar effect on the *tatABC* deletion (Fig. 2B). It is possible that fosfomycin also induces a similar futile cycle as noted with β-lactams, but that has not been shown.

Oddly, while we were able to transform pSecSP–AmiA, pSecSP–AmiC and pSecSP–SufI into the Δ*tatABC* background, we were unable to get transformants in the wild-type background after repeated attempts. Previous studies show that pBAD33 promoter is uninduced in LB without arabinose (Guzman *et al.* 1995) and we performed growth curves to verify it. Our data show that pSecSP–AmiA compensates for loss of Tat even when arabinose is not added to the media (Fig. S2A, Supporting Information). Thus, it seems that the constitutive level of expression of these engineered constructs is detrimental to the cell with a normally functioning Tat system, though we have no explanation for the apparent lethality. Additionally, the data show that arabinose added to the media is detrimental to the growth of S. Typhimurium as the vector control grows to a lower OD_{600} when grown with arabinose than without it (Fig. S2B, Supporting Information).

Hydrogenase deletions and Δ*mig5* do not properly maintain PMF

Single deletions of hydrogenase subunits secreted by Tat are not significantly different from wild-type 14028 (data not shown); however, we tested growth and viability of a triple hydrogenase deletion strain (Δ*hyaAB* Δ*hybABC* Δ*hydBC*) expecting that redundancy of other functional hydrogenases may compensate for single deletions. The Δ*hyaAB* Δ*hybABC* Δ*hydBC* viable plate counts show a significant decrease in viability of ~1000-fold in LB with ampicillin as compared with wild type (Fig. 4). While this is a notable decrease, it is still ~1000-fold more viable than the Δ*tatABC* strain. Deletion of *mig5* (*pslt046*) is also decreased ~10 000-fold in viability as compared with the wild type. Mig5 is a β-carbonic anhydrase that converts carbon dioxide to bicarbonate and protons, and *mig5* is located on the *Salmonella* virulence plasmid and thus is not present in *E. coli*. Carbonic anhydrases are a common target for drug discovery (Vullo *et al.* 2011). We predicted that deletion of the Tat-secreted hydrogenase subunits or *mig5* leads to a disruption of the proton gradient and PMF, which in turn decreases export via the Tat pathway and impacts delivery of AmiA, AmiC, SufI and MepK to the periplasm. To test this, we measured the Δ_Ψ of wild-type 14028, Δ*tatABC*, Δ*hyaAB* Δ*hybABC* Δ*hydBC* and Δ*mig5* using carbocyanine dye as described previously (Novo *et al.* 1999). The dye crosses the membrane efficiently when Δ_Ψ is normal and initially stains cells green. The dye aggregates as it accumulates in the cell, changing conformation and fluorescing red. The relative Δ_Ψ is established by determining the red:green MFI. If the ratio decreases, it means there is a decrease in the efficiency of dye import. The red:green MFI was determined by flow cytometry. The data from five independent runs of 10 000 events each demonstrate that wild-type 14028 has a red:green MFI of ~700 units, which indicates the normal Δ_Ψ level and accumulation of dye in the cell (Fig. 6). Wild-type 14028 was treated with CCCP to quench the reaction and indicate a disrupted Δ_Ψ. When 14028 is treated with CCCP, the MFI drops to ~200. The Δ*tatABC*, Δ*hyaAB* Δ*hybABC* Δ*hydBC* and Δ*mig5* strains show disrupted Δ_Ψ with red:green MFI values lower than that of wild-type 14028 (Fig. 6). The Δ*amiA* Δ*amiC* Δ*sufI* Δ*mepK* quadruple deletion strain also had a red:green MFI lower than that of wild-type 14028, indicating that the loss of these critical substrates has a dramatic effect on the health of the cell, including on the Δ_Ψ. Additionally, a representative histogram from one of the five independent flow cytometry runs shows the shift in red:green ratio in the deletion strains as compared with wild type (Fig. S3, Supporting Information). The combined Δ_Ψ data show an important role for hydrogenases in aerobic growth of S. Typhimurium.

These data are mirrored in Craig *et al.* (2013) where a hydrogenase triple mutant was attenuated for virulence 5-fold. Here, the authors clearly demonstrate that Tat and Tat substrates AmiA, AmiC and SufI are required for virulence in the mouse model of infection, and further show that a strain deficient in anaerobic respiration (Δ*moaDE* Δ*nrfA* Δ*frdA*) is not attenuated. Additionally, deletions of aerobic respiratory components are

significantly attenuated. Thus, Craig *et al.* show that conditions inside the animal are aerobic. This is important because the authors also demonstrate a Δ*hyaAB* Δ*hybABC* Δ*hydBC* phenotype in the mouse, suggesting that these hydrogenases are necessary for full virulence in aerobic conditions. Indeed, the translocation of Tat substrates is driven by PMF; thus, disruption of PMF likely leads to inefficient translocation of Tat substrates. The combined data from Craig *et al.* and our study suggest an important role for these hydrogenases in the maintenance of PMF during aerobic growth. The Δ*hyaAB* Δ*hybABC* Δ*hydBC* phenotype in both the animal model (Craig *et al.* 2013) and our ampicillin model is likely caused by poor translocation of Tat substrates AmiA, AmiC, SufI and MepK due to disrupted PMF. To show that the Δ*hyaAB* Δ*hybABC* Δ*hydBC* and Δ*mig5* strains are deficient in translocation of Tat substrates, we used a TorA–GFP plasmid previously described (Craig *et al.* 2013). In this construct, GFP is cloned into pBR322 and engineered to carry the signal sequence from the Tat substrate TorA. The data demonstrate (Fig. 7) that GFP is periplasmic in the wild-type 14028 background and cytoplasmic in the Δ*tatABC* background, as expected. The Δ*hyaAB* Δ*hybABC* Δ*hydBC* and Δ*mig5* strains show clear GFP localization to the cytoplasm, similar to the Δ*tatABC* background. This confirms that the Δ*hyaAB* Δ*hybABC* Δ*hydBC* and Δ*mig5* strains are deficient in translocation of Tat substrates to the periplasm due to the changes in Δ_ψ of these strains.

Together, these data demonstrate the importance of Tat system in the *Salmonella* response to peptidoglycan targeting antibiotics. Our results indicate that MepK, AmiA, AmiC and SufI are critical periplasmic proteins and loss of these enzymes leaves the bacterium exceptionally sensitive to antibiotics that target peptidoglycan synthesis. Further, deletions of hydrogenase subunits and the Mig5 carbonic anhydrase alter the Δ_ψ of the cell and impact delivery of MepK, AmiA, AmiC and SufI to the periplasm, leaving the cell sensitive to cell wall targeting antibiotics. We have also demonstrated the importance of these hydrogenases and Mig5 in contributing to the PMF of *Salmonella*. There are notable differences between the Tat systems of *E. coli* and *Salmonella*, including the translocation of Mig5, which is not present in *E. coli*. The Tat system is an attractive target for identification of new antimicrobial compounds. Our data show that drugs targeting the Tat system or the hydrogenases that power it could be used in combination with β-lactams to increase microbial killing capacity and could potentially extend the spectrum of existing β-lactams.

ACKNOWLEDGEMENTS

Neither the GRFC committee nor the National Institutes of Health (NIH) had any role in experimental design, data collection, interpretation or publication of this work. We would like to thank James Slauch for generously sharing strains and for helpful discussions.

SUPPLEMENTARY DATA

Supplementary data are available at FEMSMC online.

FUNDING

This work was supported by Grants and Research Funding Committee from the Southeast Missouri State University (JRE) and the National Institutes of Health Award 1R03AI144661-01 (JRE).

Conflict of Interest. None declared.

REFERENCES

Alami M, Trescher D, Wu L-F *et al.* Separate analysis of twin-arginine translocation (Tat)-specific membrane binding and translocation in *Escherichia coli*. *J Biol Chem* 2002;**277**:20499–503.

Berks BC, Palmer T, Sargent F. The Tat protein translocation pathway and its role in microbial physiology. *Adv Microb Physiol* 2003;**47**:187–254.

Berks BC, Sargent F, Palmer T. The Tat protein export pathway. *Mol Microbiol* 2000;**35**:260–74.

Berks BC. A common export pathway for proteins binding complex redox cofactors? *Mol Microbiol* 1996;**22**:393–404.

Bernhardt TG, De Boer PAJ. The *Escherichia coli* amidase AmiC is a periplasmic septal ring component exported via the twin-arginine transport pathway. *Mol Microbiol* 2003;**48**:1171–82.

Brown ED, Vivas EI, Walsh CT *et al.* MurA (MurZ), the enzyme that catalyzes the first committed step in peptidoglycan biosynthesis, is essential in *Escherichia coli*. *J Bacteriol* 1995;**177**:4194–7.

Caldelari I, Mann S, Crooks C *et al.* The Tat pathway of the plant pathogen *Pseudomonas syringae* is required for optimal virulence. *Mol Plant Microbe Interact* 2006;**19**:200–12.

Chen YC, Li CL, Hsiao YY *et al.* Structure and function of TatD exonuclease in DNA repair. *Nucleic Acids Res* 2014;**42**:10776–85.

Cherepanov PP, Wackernagel W. Gene disruption in *Escherichia coli*: tcR and KmR cassettes with the option of Flp-catalyzed excision of the antibiotic-resistance determinant. *Gene* 1995;**158**:9–14.

Chodisetti PK, Reddy M. Peptidoglycan hydrolase of an unusual cross-link cleavage specificity contributes to bacterial cell wall synthesis, *Proc Natl Acad Sci USA* 2019;**116**:7825–30.

Cho H, Uehara T, Bernhardt TG. Beta-lactam antibiotics induce a lethal malfunctioning of the bacterial cell wall synthesis machinery. *Cell* 2014;**159**:1300–11.

Craig M, Sadik AY, Golubeva YA *et al.* Twin-arginine translocation system (*tat*) mutants of *Salmonella* are attenuated due to envelope defects, not respiratory defects. *Mol Microbiol* 2013;**89**:887–902.

Datsenko KA, Wanner BL. One-step inactivation of chromosomal genes in *Escherichia coli* K-12 using PCR products. *Proc Natl Acad Sci USA* 2000;**97**:6640–5.

DeLisa MP, Lee P, Palmer T *et al.* Phage shock protein PspA of *Escherichia coli* relieves saturation of protein export via the Tat pathway. *J Bacteriol* 2004;**186**:366–73.

Edwards RA, Helm RA, Maloy SR. Increasing DNA transfer efficiency by temporary inactivation of host restriction. *BioTechniques* 1999;**26**:892–900.

Fujimoto M, Goto R, Hirota R *et al.* Tat-exported peptidoglycan amidase-dependent cell division contributes to *Salmonella* Typhimurium fitness in the inflamed gut. *PLoS Pathog* 2018;**14**:e1007391.

Gal-Mor O, Boyle EC, Grassl GA. Same species, different diseases: how and why typhoidal and non-typhoidal *Salmonella enterica* serovars differ. *Front Microbiol* 2014;**5**:391.

Gohlke U, Pullan L, McDevitt CA *et al.* The TatA component of the twin-arginine protein transport system forms channel complexes of variable diameter. *Proc Natl Acad Sci USA* 2005;**102**:10482–6.

Guzman L-M, Belin D, Carson MJ *et al.* Tight regulation, modulation, and high-level expression by vectors containing the arabinose pBAD promoter. *J Bacteriol* 1995;**177**:4121–30.

Heidrich C, Templin MF, Ursinus A *et al*. Involvement of N-acetylmuramyl-L-alanine amidases in cell separation and antibiotic-induced autolysis of *Escherichia coli*. *Mol Microbiol* 2001;**41**:167–78.

Ize B, Stanley NR, Buchanan G *et al*. Role of the *Escherichia coli* Tat pathway in outer membrane integrity. *Mol Microbiol* 2003;**48**:1183–93.

Jack RL, Sargent F, Berks BC *et al*. Constitutive expression of *Escherichia coli tat* genes indicates an important role for the twin-arginine translocase during aerobic and anaerobic growth. *J Bacteriol* 2001;**183**:1801–4.

Krueger AL, Greene SA, Barzilay EJ *et al*. Clinical outcomes of nalidixic acid, ceftriaxone, and multidrug-resistant nontyphoidal *Salmonella* infections compared with pansusceptible infections in FoodNet sites, 2006–2008. *Foodborne Pathog Dis* 2014;**11**:335–41.

Lavander M, Ericsson SK, Bröms JE *et al*. The twin arginine translocation system is essential for virulence of *Yersinia pseudotuberculosis*. *Infect Immun* 2006;**74**:1768–76.

Leake MC, Greene NP, Godun RM *et al*. Variable stoichiometry of the TatA component of the twin-arginine protein transport system observed by *in vivo* single-molecule imaging. *Proc Natl Acad Sci USA* 2008;**105**:15376–81.

Maloy S, Stewart V, Taylor R *et al*. *Genetic Analysis of Pathogenic Bacteria*. New York: Cold Spring Harbor Laboratory Press, 1996.

Mastroeni P, Grant AJ. Spread of *Salmonella enterica* in the body during systemic infection: unravelling host and pathogen determinants. *Expert Rev Mol Med* 2011;**13**:e12.

Mather AE, Reid SWJ, Maskell DJ *et al*. Distinguishable epidemics of multidrug-resistant *Salmonella* Typhimurium DT104 in different hosts. *Science* 2013;**341**:1514–7.

Nair DVT, Venkitanarayanan K, Kollanoor Johny A. Antibiotic-resistant *Salmonella* in the food supply and the potential role of antibiotic alternatives for control. *Foods (Basel, Switzerland)* 2018;**7**:167.

Novo D, Perlmutter NG, Hunt RH *et al*. Accurate flow cytometric membrane potential measurement in bacteria using diethyloxacarbocyanine and a ratiometric technique. *Cytometry* 1999;**35**:55–63.

Orriss GL, Tarry MJ, Ize B *et al*. TatBC, TatB, and TatC form structurally autonomous units within the twin arginine protein transport system of *Escherichia coli*. *FEBS Lett* 2007;**581**:4091–7.

Palmer T, Berks BC. The twin-arginine translocation (Tat) protein export pathway. *Nat Rev Microbiol* 2012;**10**:483–96.

Palmer T, Sargent F, Berks BC. Export of complex cofactor-containing proteins by the bacterial Tat pathway. *Trends Microbiol* 2005;**13**:175–80.

Pradel N, Delmas J, Wu LF *et al*. Sec- and Tat-dependent translocation of β-lactamases across the *Escherichia coli* inner membrane. *Antimicrob Agents Chemother* 2009;**53**:242–8.

Reynolds MM, Bogomolnaya L, Guo J *et al*. Abrogation of the twin arginine transport system in *Salmonella enterica* serovar Typhimurium leads to colonization defects during infection. *PLoS One* 2011;**6**:e15800.

Rollauer SE, Tarry MJ, Graham JE *et al*. Structure of the TatC core of the twin-arginine protein transport system. *Nature* 2012;**492**:210–4.

Samaluru H, Saisree L, Reddy M. Role of SufI (FtsP) in cell division of *Escherichia coli*: evidence for its involvement in stabilizing the assembly of the divisome. *J Bacteriol* 2007;**189**:8044–52.

Sargent F, Berks BC, Palmer T. The Tat protein export pathway. *EcoSal Plus* 2010;**4**:1–35.

Stanley NR, Findlay K, Berks BC *et al*. *Escherichia coli* strains blocked in Tat-dependent protein export exhibit pleiotropic defects in the cell envelope. *J Bacteriol* 2001;**183**:139–44.

Stolle P, Hou B, Brüser T. The Tat substrate CueO is transported in an incomplete folding state. *J Biol Chem* 2016;**291**:13520–8.

Tarry M, Arends SJR, Roversi P *et al*. The *Escherichia coli* cell division protein and model Tat substrate SufI (FtsP) localizes to the septal ring and has a multicopper oxidase-like structure. *J Mol Biol* 2009;**386**:504–19.

Tullman-Ercek D, DeLisa MP, Kawarasaki Y *et al*. Export pathway selectivity of *Escherichia coli* twin arginine translocation signal peptides. *J Biol Chem* 2007;**282**:8309–16.

Vullo D, Nishimori I, Minakuchi T *et al*. Inhibition studies with anions and small molecules of two novel β-carbonic anhydrases from the bacterial pathogen *Salmonella enterica* serovar Typhimurium. *Bioorg Med Chem Lett* 2011;**21**:3591–5.

Yahr TL, Wickner WT. Functional reconstitution of bacterial Tat translocation *in vitro*. *EMBO J* 2001;**20**:2472–9.